ECS Journal of Solid State Science and Technology, 2022 **11** 103007
2162-8777/2022/11(10)/103007/4/$40.00 © 2022 The Electrochemical Society ("ECS"). Published on behalf of ECS by IOP Publishing Limited

Gallium Antimonide Spherical Semiconductor Quantum Dots

Lynda Lakhal,[1,2] Fadila Mezrag,[1,z] and Nadir Bouarissa[1]

[1] *Laboratory of Materials Physics and Its Applications, Physics Department, Faculty of Science, University of M'sila, 28000, Algeria*
[2] *Physics Department, Faculty of Science, University of M'sila, 28000 M'sila, Algeria*

The quantum effects at the nano-metric level have been observed in a variety of confined structures, particularly in semiconductor quantum dots. In this contribution, the electronic and optical properties of GaSb spherical semiconductor quantum dots are investigated. For the calculations, the pseudo potential approach was employed. The size dependence of the energy gaps at Γ, X and L points, the effective masses of electrons and heavy-holes, the refractive index, and the dielectric function for a studied GaSb spherical quantum dot are analyzed and discussed. When the degree of quantum confinement effect was changed by decreasing the radius of the spherical quantum dots, a striking charge in comparison to the bulk values has been obtained. Our results indicate that as the quantum dot radius is raised, most of properties rapidly decrease. This demonstrates an improvement in the mobility of the material. However, the refractive index and the dielectric constant are increased with increasing the radius of the nano-crystal.
 [DOI: 10.1149/2162-8777/ac942e]

Manuscript submitted July 25, 2022; revised manuscript received September 5, 2022. Published October 10, 2022.

Gallium antimonide (GaSb) is a semiconductor compound made from gallium (Ga) and antimonide (Sb). It is formed of semiconductor materials in the III to V range. It has a 0.61 nm lattice constant. This lattice constant applied to the zinc-blende structure. The lattice constant's value enables its use in common semiconductor applications. The semiconductor material has a direct-band gap (Γ→Γ) with a lowest value of 0.72 eV. It has uses in lasers, transistors, infrared light emitting diodes, infrared detectors, and thermo-photovoltaic materials. It has been employed with its lattice-matched alloy systems AlGaAsSb and InGaAsSb. This was carried out in electronic devices and optoelectronics, such as hetero-junction bipolar transistors, photo-detectors, and lasers.[1–5] One should study low carrier concentration GaSb layer in order to fabricate solar GaSb-based devices. Devices based on GaSb material such as laser diodes, near infrared photodetectors, resonant tunneling structures, and other quantum devices have been reported before.[6] Moreover, the optical constants that have been obtained for the refractive index analysis the GaSb structure and its dielectric constant.

Since they can bridge the gap between bulk materials and molecular levels, nano-structured materials have attracted considerable interest.[7–13] These materials lead to novel applications avenues, particularly in biology, electronics, and optoelectronics. The last few years have seen a lot of focus on nano-structured semiconductors or quantum dots since many fundamental features depend on size in the nano-metric range. For nano-aggregated zero dimensional structures, a quantum dot has a zero dimension with respect to the bulk, and a finite number of electrons leads to discrete quantized energies in the density of states.[14–16] In fact, quantum dots exhibit properties that fall in those of bulk semiconductors and those of discrete molecules. These materials are very interesting and have applications in quantum computing, diode lasers, transistors, medical imaging, light emitting diodes and solar cells.[17]

The current presentation is focused on the electron level energies and the optical characteristics of spherical GaSb quantum dots. The pseudopotential scheme has been used for our calculations. The essential contribution of the publication is how the properties of GaSb spherical quantum dots change with the quantum dots size. The band structures and optical spectra of GaSb quantum dots are studied.The empirical pseudopotential method (EPM) is simpler in nature. It is economic and computationally precise. Moreover, this method does not underestimate the energy band-gaps. The method has shown to be efficient and produces pleasing results for the nano-scale materials.[11–13,18–20]

Computational Method

The EPM approach has been used to carry out the calculations.[21–23] For bulk GaSb, we have employed Bloch's theorem and Bloch wave functions to benefit from lattice translational symmetry. The electron's Schrödinger equation is therefore expressed as,

$$\left[\frac{P^2}{2m} + V(r)\right]\psi(r) = E\ \psi(r) \qquad [1]$$

which is subject to the boundary condition,

$$V(r) = V(r + R_n) \qquad [2]$$

Using the EPM, the atomic form factors Va(G) have been fitted to experiments. We assume that a linear superposition of the atomic potentials determines the crystal's potential V(r). The usage of a few cycles has typically resulted in agreement between theories and experiments for the optical properties, densities of state, and electronic structures. In general, it was discovered that only three form factors were necessary to accurately determine each atomic potential.

The form factors of the pseudopotential are determined by the fit of the atomic form factors. We employed a non-linear least-squares fitting procedure to make the adjustments.[24–26] The experimental energy gaps we used in this study for bulk GaSb at Γ, X and L points that we fixed in the fits are represented in Table I. Table II displays the pseudopotential form factors finally adjusted for bulk GaSb.

To investigate the GaSb quantum dots, we need to reduce the environment dimension of electrons to a zero-dimension. This leads to an energy states discretization. This gives rise to energy levels instead of energy band structures.[28] These energies levels are calculated by the improvement of the proper boundary conditions on the wave functions. These boundary conditions depend on the shape and the size of the dots, i.e.

$$k = \frac{\pi}{\sqrt{3}a}(n_x, n_y, n_z) = \frac{\pi}{\sqrt{3}a}n \qquad [3]$$

Here a indicates the radius of the spherical quantum dots.

The relation used for the effect of quantum confinement on the Eg for GaSb quantum dots is,[29,30]

$$E_g = E_g^0 + \frac{\hbar^2\pi^2}{2a^2}\left[\frac{1}{m_e^*} + \frac{1}{m_{hh}^*}\right] - \frac{1.8e^2}{\varepsilon a} \qquad [4]$$

[z] E-mail: mezrag_fadila@yahoo.fr

Table I. Experimental band-gap energies for bulk GaSb fixed in the fits. The experimental values are at 300 K.

Compound	$E_{\Gamma\text{-}\Gamma}$ (eV)	$E_{\Gamma\text{-}X}$ (eV)	$E_{\Gamma\text{-}L}$ (eV)
GaSb	0.72 [a)]	1.05 [a)]	0.76[a)]

a) Expt. Ref. 27.

Table II. Pseudopotential parameters for bulk GaSb.

Compound	Form factors (Ry)						Lattice constant (Å)
	$V_S(3)$	$V_S(8)$	$V_S(11)$	$V_A(3)$	$V_A(4)$	$V_A(11)$	
GaSb	−0.200312	0.00	0.044258	0.020435	0.045000	−0.042017	6.118

In this equation, E_g^0 is the energy gap of the bulk GaSb, m^*_e is the electron and m^*_{hh} is the heavy-hole effective masses for bulk GaSb, and ε is the effective dielectric constant. The m^*_e and m^*_{hh} are determined using a relation similar to that employed by Bouarissa.[31]

Results and Discussion

The calculated electronic structure for bulk GaSb (solid lines) and that obtained for nano-structured GaSb with a 1 nm in radius (dashed lines) are shown in Fig. 1. We used maximum valence bands as a reference for both bulk and nano-scale materials. By carefully examining the figure, one can see that the lowest of the conduction band for bulk GaSb is located at the Γ point which is at the center of the Brillouin zone, [0,0,0] π/a_0. We can conclude that the bulk GaSb compound is a direct (Γ–Γ) band-gap energy material which is consistent with experiment and theory findings.[27,32] For nano-structured GaSb, the change of the size of the material leads to the change of all the energy levels. Nevertheless, the overall shape rests the same as that of the bulk compound. The shift of all these levels has been done with various values. We observe that the lowest conduction band for GaSb quantum dots with 1 nm in radius is remained in the Γ point at the center of the Brillouin zone. As a result, the studied compound nature remains the same while scaling down from bulk to nano-scale. One may conclude that the GaSb quantum dot is a (Γ–Γ) semiconductor.

The change in the direct (Γ–Γ) energy gap for GaSb structure vs a spherical shape quantum dot radius is displayed in Fig. 2. The radius is chosen in the interval 1–10 nm. One can see that E(Γ–Γ) is decreased when we increase the radius of the quantum dot. The qualitative behavior is similar to that for nano-structured GaN[12] and InAs spherical quantum dots.[13] We can see that the decrease of the (Γ–Γ) direct band-gap is weaker and hence has tendency for retrieving the value of the bulk GaSb material. In fact, if the quantum dot size is reduced, there is an increase of the quantum confinement effect. In semiconductors, there is a Coulomb interaction which exists between electrons and holes. The interaction has essential influences on their optical characteristics. In fact, electrons and holes can be pointed together and forming excitons. In the hydrogen atom, the radius of the exciton is highly superior to that of the Bohr. This is related to the material under study. For the present work, the large bulk Bohr radius of GaSb materials was found to be higher. In fact, if the size of the quantum dot is higher than the radius of the exciton Bohr, the situation can be found similarly to that in the bulk GaSb. This is in accord with the present findings.

In Fig. 3 we depict the change in the direct gap E(Γ–Γ), as well as the indirect band gaps E(Γ–X) and E(Γ–L) of GaSb quantum dots with zinc-blende structure. Note that the energy band gaps E(Γ–Γ), E (Γ–X) and E(Γ–L) are decreased drastically and monotonically when the radius of the quantum dot is increased from 1 nm up to 10 nm. Then all of them become almost constant. Therefore, the effect of the quantum confinement was to open the band-gaps energies for radii smaller than 10 nm. The obtained values are those so called Bohr radii. The energies E(Γ–Γ), E(Γ–X) and E(Γ–L) have been obtained in the bulk to be 0.72, 1.05 and 0.76 eV, respectively. The results obtained agree satisfactorily with those cited in Ref. 27. We remark from Fig. 3 that GaSb quantum dots are always a direct gap material for the size of the nano-crystal which is situated between 1 and 10 nm. The same qualitative behavior was found for nano-structured GaAs[33] and AlN.[34] In the absence of both experiment and theory that were not reported for these quantities, the present results have been predicted and can be used as a reference.

The knowledge of the electrons and heavy-holes effective masses can give useful information on transport properties in semiconductor materials.[35] These quantities can be determined using the electronic

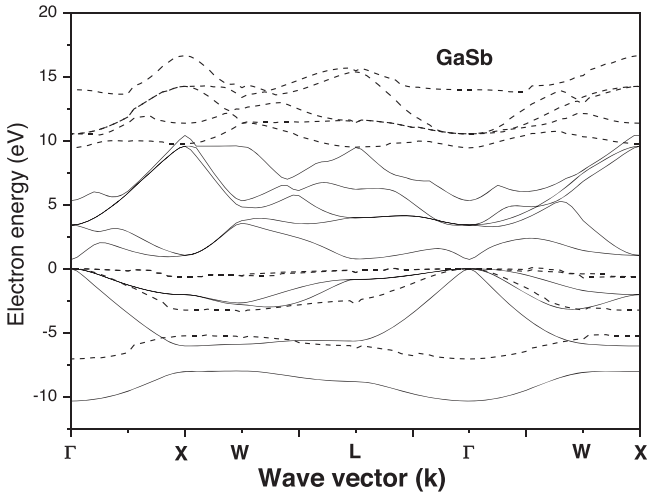

Figure 1. Electronic structure for bulk GaSb (solid lines) and electron energy levels for GaSb quantum dots with 1 nm in radius (dashed lines).

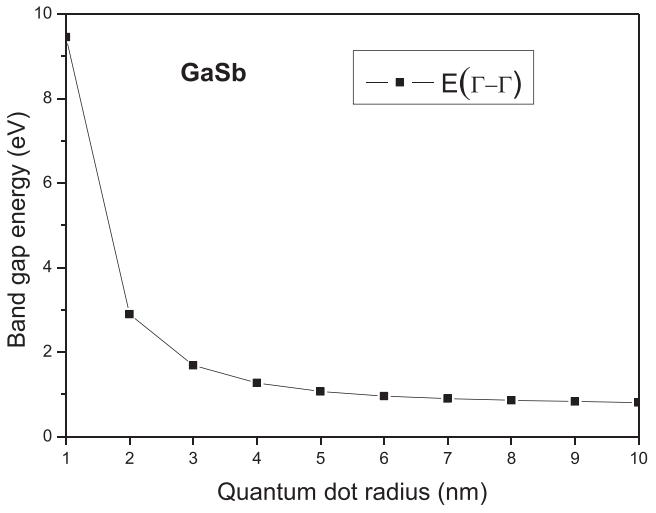

Figure 2. Direct gap (Γ–Γ) in nanosized GaSb as a function of quantum dot radius.

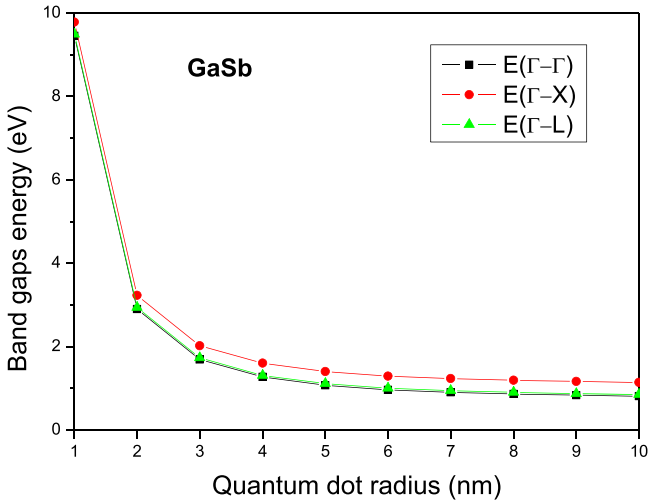

Figure 3. Direct gap (Γ–Γ) and indirect gaps (Γ–X) and (Γ–L) in nanosized GaSb vs quantum dot radius.

structure of the material under consideration. For a simple approximation, we use a parabolic E(k) dependencies that is in general used in the $A^{III}B^{V}$ semiconductors. Thus, for a unique wave vector k, the electron and heavy-hole effective masses are determined by.[36]

$$\frac{1}{m_{ij}^{*}} = \frac{4\pi^2}{h^2}\left(\frac{\partial^2 E(k)}{\partial k_i \partial k_j}\right) \quad [5]$$

and are obtained from the use of a similar procedure to that reported previously by Bouarissa.[31] For bulk GaSb, our results provide values of $m^*_e = 0.05\ m_0$ and $m^*_{hh} = 0.31\ m_0$ (in units of the free electron mass). The results agree reasonably well with those of Γ-valley, $m^*_e = 0.041\ m_0$ and $m^*_{hh} = 0.4\ m_0$ published in the literature.[37]

The variation regarding both the electron and heavy-hole effective masses at the Γ-point of the Brillouin zone vs the quantum dot radius for GaSb nano-structured material is shown in Figs. 4 and 5, respectively. Note that by increasing the radius of the quantum dot from 1 to 10 nm, m^*_e and m^*_{hh} decrease. The decrease is shown to be rapid up to a nano-crystal radius of around 5 nm then it becomes slow up to a radius of 10 nm. A non-linear variation can be seen between the m^*_e and m^*_{hh} vs the nano-crystal radius. This results in the increase of the material mobility which provides more changes for describing most transport properties.

In optics, the refractive index (n) of a material is a number without dimension which indicates how lights, or any other radiations, propagate through that material. To determine the velocity of light in such a medium, its properties are needed to be known. For electromagnetic waves, the velocity depends on the medium optical density. This is true for semiconductor materials in bulk and nanostructures.[38–40] In the present case, n is obtained in the quantum dots GaSb within a spherical shape vs a quantum dot size which ranges in the interval 1–10 nm. The following models were used to calculate n: (i) The Moss relation[41] according to Ravindra and Srivastava.[42] (ii) The Hervé and Vandamme empirical relation.[43] (iii) The Reddy and Ahammed empirical expression[44] and (iv) The Reddy and Anjaneyulu relation.[45] The results obtained from these operations are illustrated in Fig. 6. We note that when the size of the quantum dot increases, n of GaSb quantum dots increases monotonically. The result is true for all models used here. For bulk GaSb, the experiment demonstrated that the infrared refractive index n is found to be approximately 3.8.[37] This value agrees very well with our value obtained for this work using the Reddy and Anjaneyulu relation.[45] However, for a nano-crystal radius situated in 1–10 nm, when going from 10 to 1 nm, n seems to reduce with respect to that of the bulk, in particular when approaching the value of 1 nm. This is true for all employed models we have used here. The obtained

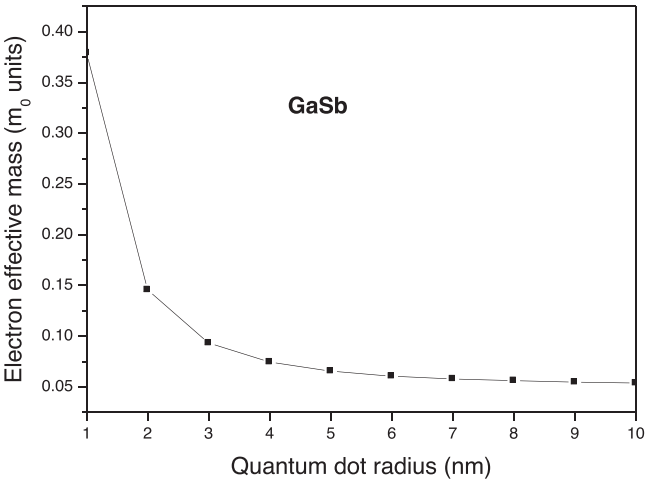

Figure 4. Electron effective mass (in m_0 units) in nanosized GaSb vs quantum dot radius.

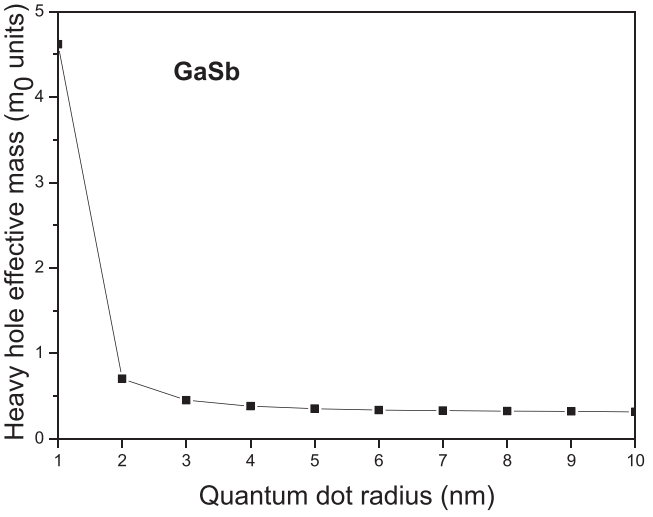

Figure 5. Heavy hole effective mass (in m_0 units) in nanosized GaSb vs quantum dot radius.

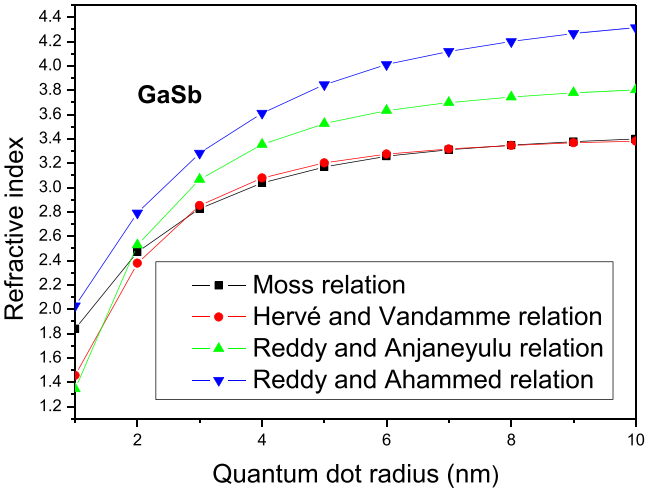

Figure 6. Refractive index in nanosized GaSb vs quantum dot radius.

results of n using the model of Reddy and Anjaneyulu[45] have been fitted using a least-squares procedure. This gives the relation,

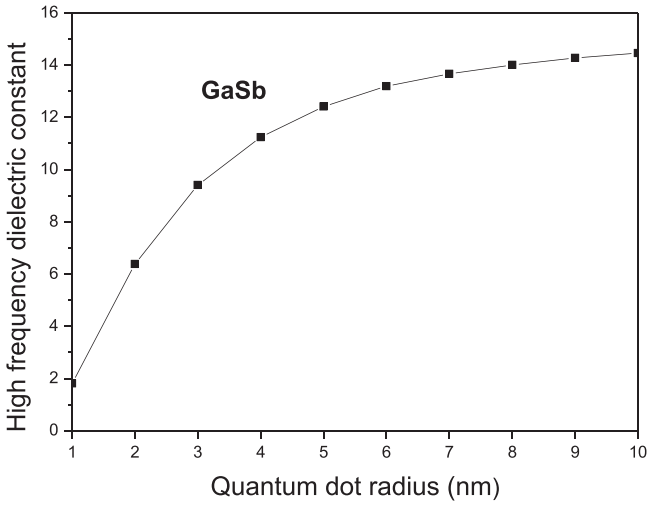

Figure 7. High-frequency dielectric constant in nanosized GaSb vs quantum dot radius.

$$n(a) = 0.98 + 0.76a - 0.05a^2 \quad [6]$$

If the permittivity of a substance is divided into that of a free space, the dielectric constant is obtained. This may indicate how easily we can polarize a material by imposing an electric field on an insulator. Generally speaking, materials with low dielectric constants are more resistant to intense electric fields than materials with high dielectric constants, which break-down easily in the presence of such fields. Thus, the greater the polarization that develops a substance in an applied field of a given strength, the higher the dielectric constant is.[46,47] In the present work, the high-frequency dielectric constant (ε_∞) is obtained from the formula Eq.7, As a result, the dielectric constant increases in proportion to the amount of polarization that a substance exhibits in an applied field of a certain strength.[46,47] The high-frequency dielectric constant (ε_∞) is calculated in the current study using the formula,

$$\varepsilon_\infty = n^2 \quad [7]$$

In Eq. 7, n represents the refractive index that which is determined from the use of formula 6. The value obtained for ε_∞ here was determined to be 14.44 for bulk GaSb. This value is in good agreement with that of 14.4 cited in.[37]

In Fig. 7, we show the variation of ε_∞ vs the radius of GaSb quantum dot. It is to be shown that by increasing the size of GaSb quantum dots, ε_∞ is increased. This shows monotonic and non-linear behavior. So, values of ε_∞ for GaSb quantum dots are inferior to those of the bulk GaSb. In fact, semiconductors which have higher dielectric constant are important materials in the manufacture of big-value capacitors and have become interesting especially in memory cell dielectrics, passive components and gate dielectrics. By fitting data regarding ε_∞, we will obtain,

$$\varepsilon_\infty(a) = -0.72 + 3.78a - 0.23a^2 \quad [8]$$

We can note from Eq. 8 that ε_∞ varies non-linearly and shows a bowing parameter of −0.23.

Conclusion

In conclusion, the electronic band structure of GaSb spherical quantum dots has been examined, including the energy gaps, electronic and heavy-hole effective masses, refractive index and the high-frequency dielectric constant. Using a pseudopotential approach, the calculations were performed. It has been reported that all quantities of interest are affected by the quantum confinement effect. The direct band-gap E(Γ–Γ) and indirect energy gaps E(Γ–X) and E(Γ–L) were found to be decreased when going from 1 up to 5 nm. Their effective masses were diminished monotonically when we increase the quantum dot radius up to 5 nm. For quantum dots with a radius between 5 and 10 nm, the band-gap energies and effective masses are nearly constant. The decrease of the carrier's effective masses can increase their mobility's. The refractive index and the high frequency dielectric constant were increased when the quantum dot radius was increased in the range of 1–5 nm. These quantities displayed a little rise when the quantum dot radius was between 5 and 10 nm.

ORCID

Fadila Mezrag https://orcid.org/0000-0001-6970-3191
Nadir Bouarissa https://orcid.org/0000-0003-0520-4099

References

1. A. G. Milnes and A. Y. Polyakov, *Solid-State Electron.*, **36**, 803 (1993).
2. J. O. Akinlami, *Res. J. Phys.*, **8**, 17 (2014).
3. S. Adachi, "Optical constants of crystalline and amorphous semiconductors." *Numerical Data and Graphical Information* (Springer)(New York) (1999) .
4. N. Bouarissa, *Phys. Lett. A*, **245**, 285 (1998).
5. K. Kassali and N. Bouarissa, *Microelectron. Eng.*, **54**, 277 (2000).
6. I. Vurgaftman, J. R. Meyer, and L. R. Ram-Mohan, *J. Appl. Phys.*, **89**, 5815 (2001).
7. L. Venema, *Nature*, **442**, 994 (2006).
8. L. E. Brus, *IEEE J. Quantum Electron.*, **22**, 1909 (1986).
9. P. Harrison, *Quantum Wells, Wires and Dots: Theoretical and Computational Physics* (Wiley, New York) (2000).
10. C. Q. Sun, *Prog. Solid State Chem.*, **35**, 1 (2007).
11. N. Bouarissa, *J. Comput. Theor. Nanoscience*, **10**, 1284 (2013).
12. A. Gueddim, T. Eloud, N. Messikine, and N. Bouarissa, *Superlatt. Microstruct.*, **77**, 124 (2015).
13. F. Mezrag, N. Bouarissa, and M. Boucenna, *Optik*, **127**, 1167 (2016).
14. K. E. Andersen, C. Y. Fong, and W. E. Pickett, *J. Non-Cryst. Solids*, **299**, 1105 (2002).
15. R. C. Ashoori, *Nature*, **379**, 413 (1996).
16. C. B. Murray, C. R. Kagan, and M. G. Bawendi, *Ann. Rev. Mater. Sci.*, **30**, 545 (2000).
17. H. Y. Ramirez, J. Flórez, and A. S. Camacho, *Phys. Chem. Chem. Phys.*, **17**, 23938 (2015).
18. G. Bester, *J. Phys. Condens. Matter*, **21**, 023202 (2009).
19. P. R. C. Kent, L. Bellaiche, and A. Zunger, *Semicond. Sci. Technol.*, **17**, 851 (2002).
20. D. Bera, L. Qian, T.-K. Tseng, and P. H. Holloway, *Materials*, **3**, 2260 (2010).
21. M. L. Cohen and J. R. Chelikowsky, *Electronic Structure and Optical Properties of Semiconductors* (Springer, Berlin, Heidelberg) (1988).
22. R. M. Martin, *Electronic Structure: Basic Theory and Practical Methods* (Cambridge University Press, Cambridge) (2004).
23. N. Bouarissa, *Mater. Chem. Phys.*, **65**, 107 (2000).
24. T. Kobayasi and H. Nara, *Bull. Coll. Med. Sci. Tohoku Univ.*, **2**, 7 (1993).
25. N. Bouarissa and M. Boucenna, *Phys. Scr.*, **79**, 015701 (2009).
26. N. Bouarissa, *Mater. Chem. Phys.*, **124**, 336 (2010).
27. S. Adachi, *Properties of Group-IV, III-V and II-VI Semiconductors* (Wiley, New York) (2005).
28. A. Kshirsagar and N. Kumbhojkar, *Bull. Mater. Sci.*, **31**, 297 (2008).
29. Y. Kayanuma, *Phys. Rev. B*, **38**, 9797 (1988).
30. R. Ragan, "Direct energy band gap group IV alloys and nanostructures." *PhD Dissertation*, (Pasadena)California Institute of Technology (2002).
31. N. Bouarissa, *J. Phys. Chem. Solids*, **67**, 1440 (2006).
32. N. Bouarissa, *Mater. Chem. Phys.*, **100**, 41 (2006).
33. N. H. M. AlWadiy, N. Bouarissa, and M. A. Khan, *Phys. Scr.*, **84**, 015704 (2011).
34. A. Hafaiedh and N. Bouarissa, *Physica E*, **43**, 1638 (2011).
35. D. L. Rode, "Semiconductors and semimetals.", ed. R. K. Willardson and A. C. Beer *Transport Phenomena* (Academic, New York) 10, 1 (1975).
36. W. Nakwaski, *Physica B*, **210**, 1 (1995).
37. M. Levinshtein, S. Rumyantsev, and M. Shur (ed.), *Handbook Series on Semiconductor Parameters* (World Scientific, Singapore) 1 (1996).
38. N. Bouarissa, *Mater. Chem. Phys.*, **72**, 387 (2001).
39. F. Mezrag and N. Bouarissa, *Mater. Res.*, **22**, e20171146 (2019).
40. F. Benmakhlouf, A. Bechiri, and N. Bouarissa, *Solid-State Electron.*, **47**, 1335 (2003).
41. T. S. Moss, *Proceedings of the Physical Society, section B*, **63**, 167 (1950).
42. N. M. Ravindra and V. K. Srivastava, *Infrared Phys.*, **19**, 605 (1979).
43. P. Hervé and L. K. J. Vandamme, *Infrared Phys. Technol.*, **35**, 609 (1994).
44. R. R. Reddy and Y. N. Ahammed, *Infrared Phys. Technol.*, **36**, 825 (1995).
45. R. R. Reddy and S. Anjaneyulu, *Phys. Stat. Sol. B*, **174**, K91 (1992).
46. A. Gueddim, S. Zerroug, and N. Bouarissa, *J. Lumin.*, **135**, 243 (2013).
47. S. Ferahtia, S. Saib, N. Bouarissa, and S. Benyettou, *Superlatt. Microstruct.*, **67**, 88 (2014).